



## Short communication

## Efficient detection of localized corrosion processes on stainless steel by means of scanning electrochemical microscopy (SECM) using a multi-electrode approach

Marco Hampel<sup>a</sup>, Matthias Schenderlein<sup>a</sup>, Christian Schary<sup>a,b</sup>, Matthias Dimper<sup>a</sup>, Ozlem Ozcan<sup>a,\*</sup><sup>a</sup> Federal Institute for Materials Research and Testing (BAM), Unter den Eichen 87, Berlin 12205, Germany<sup>b</sup> Beuth University of Applied Sciences Berlin, Luxemburger Str. 10, Berlin 13353, Germany

## ARTICLE INFO

## Keywords:

Pitting corrosion  
 Stainless steel  
 Scanning electrochemical microscopy (SECM)  
 Multi-electrode arrays  
 Corrosion sensing

## ABSTRACT

High resolution analysis of corrosion processes on stainless steels is a challenging task. The application of local electrochemical techniques such as scanning electrochemical microscopy (SECM) has opened new possibilities for the detection of corrosion products and activity on metallic surfaces. However, due to its stochastic nature, the analysis of pitting corrosion requires being at the right place at the right time. Scanning over large areas at a high resolution not only leads to long scan durations but also leaves many short-lived processes undetected. In this paper we present the combined automated operation of SECM and wire multi-electrodes connected to a multi-electrode analyzer (MMA). The inter-electrode currents between 25 wire electrodes connected via zero resistance ammeters (ZRA) are measured by the MMA at open circuit potential (OCP) and the electrodes reporting anodic currents are detected automatically to be analyzed by means of SECM. The results demonstrate the successful application of this methodology for the detection of unstable and stable pitting processes on 304 stainless steel in a corrosive aqueous environment.

## 1. Introduction

The analysis of electrochemical reactions on surfaces with a high spatial resolution has become available with the introduction of scanning electrochemical microscopy by Bard et al. [1], and has since been applied for the analysis of a great variety of electrochemical processes [2,3,4,5,6]. With the possibility of detection of diverse reactive species and corrosion products, SECM is a vital tool for corrosion research. The challenge of applying SECM to corrosion studies for materials susceptible to local corrosion is the difficulty in predicting where the processes will occur. The size of the scan area and the desired spatial resolution determine the scan duration, which is very critical considering the dynamic nature of the local corrosion processes.

The passive film breakdown and pit nucleation on 304 and 316 stainless steels was studied by Izquierdo et al. in chloride containing acidic media by the detection of  $\text{Fe}^{2+}$  and  $\text{Fe}^{3+}$  species [7,8]. They have used polarization and galvanic coupling of the two materials to initiate pitting corrosion. Aouina et al. has applied SECM to initiate and investigate single pits on 316L austenitic stainless steel by the local release of  $\text{Cl}^-$  ions from the probe [9]. Schuhmann and co-workers have utilized constant-distance mode of AC-SECM for the elucidation of

the pit initiation on 316 Ti stainless steel by using the SECM probe as the counter electrode for the polarization experiment [10]. As an alternative approach, galvanostatic polarization was used to trigger pitting corrosion in a 0.1 M NaCl solution at natural pH by Yin et al. [11]. Corrosion processes on metals more prone to corrosion like pure iron or magnesium alloys can be investigated at OCP conditions just by adjusting the corrosive load [12,13]. In recent studies, simultaneous chemical mapping and combination of chemical sensing with local pH measurements was demonstrated for different bimetallic galvanic couples by the operation of an SECM using double-barrel probes combining ion selective microelectrodes (ISME) and pH electrodes [14,15,16].

Another established method for corrosion research, besides SECM, is the use of coupled multi-electrode arrays (MEA). MEAs are arrays of electrodes that are electrically isolated towards the electrolyte side but are connected via zero resistance ammeters to allow galvanic coupling to simulate a macroscopic material surface [17,18,19]. They allow the monitoring of inter-electrode currents between individual electrodes and thus the determination of pitting probability and the active electrodes in a corrosive environment [17].

In the present study, the advantages of coupled MEAs in terms of corrosion sensing are combined with the electrochemical analysis by

\* Corresponding author.

E-mail address: [ozlem.ozcan@bam.de](mailto:ozlem.ozcan@bam.de) (O. Ozcan).

means of SECM. In this proof of concept study, the detection of electrodes with an anodic overall current and subsequent scanning by means of SECM in a chloride containing acidic electrolyte was demonstrated under OCP conditions for 304 stainless steel.

## 2. Experimental

All given potentials refer to an Ag/AgCl (3 M NaCl) reference electrode (RE-3VT by ALS Co. Ltd., Japan). All Solutions were prepared using analytical grade chemicals and de-ionized water (0.055  $\mu$  S/cm, Evoqua, USA).

### 2.1. Preparation of coupled MEAs

For the construction of MEAs 304 stainless steel wires of 0.5 mm diameter (Goodfellow GmbH, Germany) have been degreased for 5 min in an ultrasonic bath in a 1:1 mixture of acetone/ethanol and were subsequently embedded in an epoxy matrix using two masks with predrilled holes for uniform separation. The free ends of the wires were soldered to ribbon cables with connectors for convenience. The assembly was cut in half to obtain two symmetrical MEAs. Sample surfaces were polished plane up to P4000 grit size with SiC paper and cleaned in an ultrasonic bath in water and acetone/isopropanol (1:1) for 5 min each.

### 2.2. Procedure of combined MMA-SECM operation

The automatic operation requires a precise determination of the electrode positions for maneuvering the SECM probe. For all experiments the 25 wire electrodes were connected to a multichannel microelectrode analyzer (MMA Model 900B with 1  $\mu$  A modules, Scribner Associates Inc., USA) in the zero-resistance ammeter (ZRA) mode. The SECM setup was a M470 ac/dc-SECM (BioLogic, France), operated using a 10  $\mu$  m Pt probe (Uniscan Instruments, UK). Tip to substrate distance was established by recording approach curves at three different positions at the corners of a triangle outside of the MEA area to assure a tilt free operation.

For the determination of electrode positions, two different modes were tested in 1 mM KCl: The first is operating the SECM in ac-mode where a shift in the current phase between conductive electrodes and insulating epoxy resin is observed (data not shown). The second is the redox competition mode for oxygen reduction where MEA and the Pt-SECM probe are both polarized at  $-0.65$  V. The oxygen consumption takes place only on wire electrodes and results in a clear contrast with the insulating matrix as seen in Fig. 1A. Both modes provide reliable results for the determination of the electrode positions.

Based on the measurements, the center points of the wire electrodes have been determined and a scan area of  $700 \times 700 \mu\text{m}$  around each individual electrode was defined to assure reproducible maneuvering. For the corrosion experiment, the MEA was kept at OCP in 0.25 M NaCl electrolyte at pH 2. The Pt-SECM probe was polarized to 0.45 V and the SECM was operated in SG/TC mode for the detection of  $\text{Fe}^{2+}$  ions.

After one day monitoring at OCP,  $\text{H}_2\text{O}_2$  was added to the electrolyte in two steps to a final concentration of 0.003% (vol.) to trigger stable pitting for testing the detection procedure. The duration of one SECM scan of  $700 \times 700 \mu\text{m}$  area was 47 min with 15 min between scans to let the system settle down before the next scan position is determined.

## 3. Results and discussion

As seen in Fig. 2A, in the first hours of the corrosion experiment only small current spikes were observed in the current traces by means of the MMA. In the SECM scans that were conducted while the MMA did not indicate pitting, no  $\text{Fe}^{2+}$  signal was detected. As seen in Fig. 1B, during the simultaneous operation of SECM and MMA, the scanning process induces a  $-100$  to  $-150$  mV cathodic shift of the base

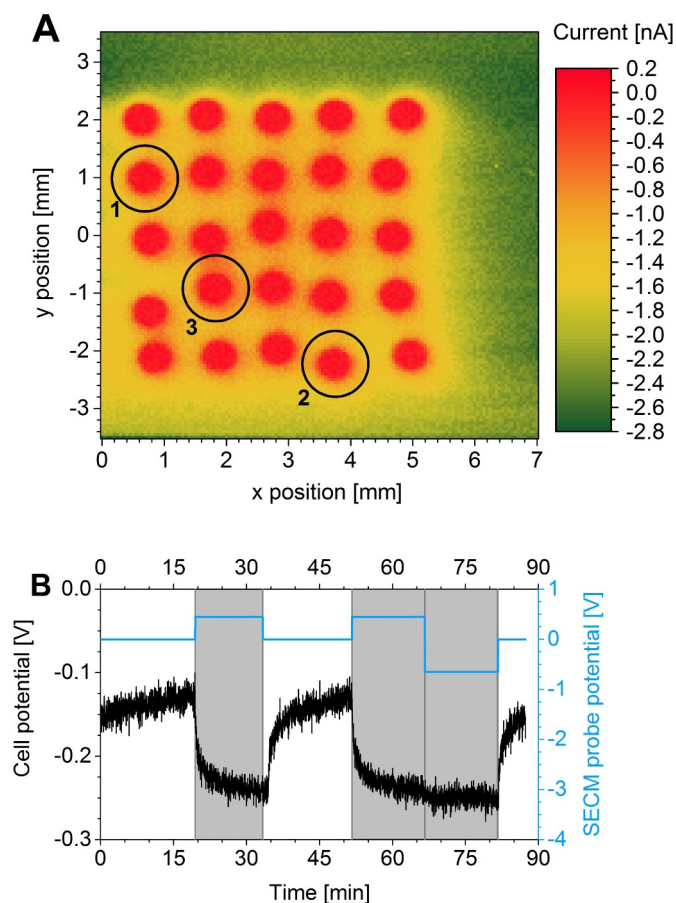


**Fig. 1.** A: SECM area scan of multi-electrode array to identify exact coordinates of single electrodes. The numbering of the marked electrodes corresponds to the numbering in Fig. 2A of the electrodes reporting anodic currents. B: Measurement showing the cathodic shift in the potential of the multi-electrode array (black line) induced by polarization of the SECM probe (grey zones, blue line). (For interpretation of the references to color in this figure legend, the reader is referred to the web version of this article.)

potential of the electrode array independent of the amplitude or sign of the polarization potential of the SECM probe. The current trace data also indicates that the noise of the signal is higher during the SECM scans. During the waiting times between the SECM scans, where the SECM probe is operated at its OCP, the base potential returns to its initial value resulting in a sudden anodic shift. The highest base potential levels achieved in the waiting periods are around 0 V which is significantly below the pitting potential of 304 stainless steel under these conditions. Nevertheless, this sudden return of the base potential due to the crosstalk between two setups enables spontaneous pitting processes to be observed. The first such unstable pit was detected by means of the MMA after four and a half hours on the electrode 1.2 (indicated with 1 in Figs. 1A and 2A). The successive SECM mapping clearly localized the pitting process (Fig. 2B). According to the MMA current trace data pit 1 repassivated within 30 minutes during the first SECM scan and the consecutive SECM map on the same electrode has shown no  $\text{Fe}^{2+}$  signal (data not shown). The same electrode (1.2) initiated a second pitting process after 21 h, which was also successfully detected by the automated recognition via MMA current trace as seen in Fig. 2C. In the next scan shown in Fig. 2D, however, the active area was repassivated until the scan reached that location and the SECM scan was not able to catch the active state.

With the current state of the recognition routine, the electrode that has the highest anodic signal at the time when the MMA data are read out, is selected for the next SECM area scan. The pitting process on

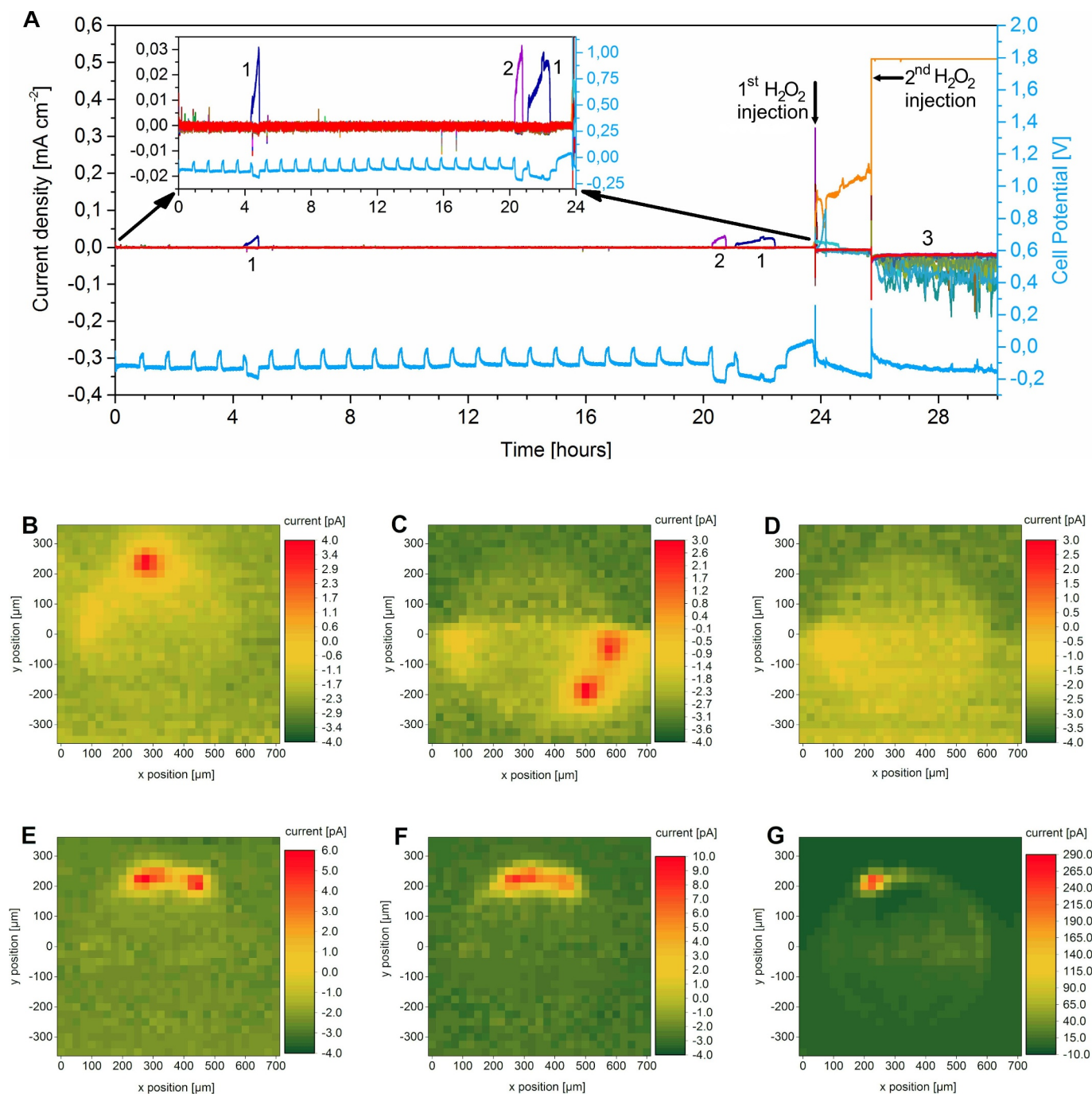


**Fig. 2.** A: MMA-readings of the current densities of all 25 electrodes of the multi-electrode array during the run of the experiment. The numbers 1–3 in the graph indicate 3 individual electrodes that showed corrosion, the numbers correspond to Fig. 1A. The blue graph at the bottom shows the reading of the multi-electrode's potential, where regular cathodic polarizations corresponding to SECM scans can be identified. The inset in the upper left shows a close-up of the OCP monitoring period in 0.25 M NaCl (pH 2). B: SECM area scan of electrode 1.2 during pitting after ~4.5 h. C: SECM area scan of electrode 1.2 during pitting after ~21 h. D: SECM area scan of an electrode where no definite corrosion signal was detected because it repassivated before the scan was finished. E and F: Two consecutive SECM area scan of electrode 4.5 after first injection of H<sub>2</sub>O<sub>2</sub> showing signals of corrosion. G: SECM area scan of electrode 4.5 after the second injection of H<sub>2</sub>O<sub>2</sub> showing high anodic current. (For interpretation of the references to color in this figure legend, the reader is referred to the web version of this article.)

electrode 4.5 (indicated with 2 in the current trace data in Fig. 2A), occurred during the scan of another electrode and thus was not scanned by SECM.

After the observation of unstable pitting processes for 24 h, H<sub>2</sub>O<sub>2</sub> was added to the electrolyte to initiate stable pitting to test the recognition routine and to evaluate the applicability of the setup for future studies on the effect of different corrosive agents and corrosion inhibitors. After the addition of the first drop of H<sub>2</sub>O<sub>2</sub> solution, the cell

potential continuously rose to 0 V at first and spiked to 0.28 V after the addition of the full concentration to reach 0.003 vol%. After the spike, the electrode 2.4 (indicated as 3 in the current trace in Fig. 2A) became active and the current levels rose to the detection limit of MMA. The two consecutive scans after the first injection are presented in Fig. 2E and F, where the increase in Fe<sup>2+</sup> signal has been observed with values 2–3 times higher than the ones observed in the unstable pitting processes without the addition of H<sub>2</sub>O<sub>2</sub>. After the second injection, the

$\text{Fe}^{2+}$  signal reached 290 pA (Fig. 2G). The recognition routine stably selected this electrode for the rest of the experiment and the current levels stayed nearly constant for the next 24 h. Interestingly, the anodic spikes observed during the waiting periods were not pronounced after the addition of  $\text{H}_2\text{O}_2$ . The crosstalk between the two setups resulting in cathodic shift of the base potential of the array electrode disappears as the inter-electrode current flow increases due to the increased corrosive load. The clarification of the mechanisms leading to the crosstalk is the topic of ongoing work. One possible explanation that is currently being tested is the presence of electrical field effects. It has been recently reported for potentiometric SECM operation that double-barrel SECM probes combining an ion selective microelectrode (ISME) with an internal reference electrode can avoid signal artefacts induced by potential fields [16,20]. Nevertheless, considering that the crosstalk leads to a cathodic shift with a non-critical magnitude, the unintentional pulsing of the potential might be useful in probing pitting behavior of different materials without the need of deliberate polarization of one selected electrode into the pitting regime.

#### 4. Conclusions

With this paper we present the combination of SECM with a MMA for the investigation of localized corrosion processes under OCP conditions. The setup provides an efficient tool with high sensitivity for localization of corrosion sites without the need for external triggering or corrosion initiation, which interfere with the stochastic nature of the pitting processes. Moreover, the precise and automated maneuvering of the SECM mapping and the resulting reduction of the area of the analysis increases the time resolution of the SECM analysis significantly.

In this proof of concept study, the developed methodology was applied to the localized corrosion of 304 stainless in chloride containing acidic media. However, it can easily be adapted to a nearly all materials relevant to corrosion to investigate corrosion mechanisms, effects of galvanic coupling and for testing the efficiency of corrosion inhibitors. Moreover, with the great flexibility that SECM offers regarding detection of chemical species, it can be used to study surface reactions, where electrochemical activity is intended to be correlated with the local chemical environment.

#### Acknowledgments

The authors greatly acknowledge the financial support from the PhD Program of the Federal Institute for Materials Research and Testing (BAM), Germany (M. Hampel) and the ZIM Project il-KDM (ZF4044205WM6) funded by the German Federal Ministry for Economic Affairs and Energy (M. Schenderlein).

#### References

[1] A.J. Bard, F.R.F. Fan, J. Kwak, O. Lev, Scanning electrochemical microscopy.

- Introduction and principles, *Anal. Chem.* 61 (2) (1989) 132–138.
- [2] M. Zhao, Z. Qian, R. Qin, J. Yu, Y. Wang, L. Niu, In situ SECM study on concentration profiles of electroactive species from corrosion of stainless steel, *Corros. Eng. Sci. Technol.* 48 (4) (2013) 270–275.
- [3] R.M. Souto, A. Kiss, J. Izquierdo, L. Nagy, I. Bitter, G. Nagy, Spatially-resolved imaging of concentration distributions on corroding magnesium-based materials exposed to aqueous environments by SECM, *Electrochem. Commun.* 26 (2013) 25–28.
- [4] H. Skiku, T. Shiraishi, H. Ohya, T. Matsue, H. Abe, H. Hoshi, M. Kobayashi, Monitoring activity of living cells entrapped in a membrane-sealed microcapillary with scanning electrochemical microscopy, *Electrochemistry* 68 (11) (2000) 890–892.
- [5] R. Schaller, S. Thomas, N. Biribilis, J. Scully, Spatially resolved mapping of the relative concentration of dissolved hydrogen using the scanning electrochemical microscope, *Electrochem. Commun.* 51 (2015) 54–58.
- [6] G. Wittstock, M. Burchardt, S.E. Pust, Y. Shen, C. Zhao, Scanning electrochemical microscopy for direct imaging of reaction rates, *Angew. Chem. Int. Ed.* 46 (10) (2007) 1584–1617.
- [7] J. Izquierdo, L. Martín-Ruiz, B. Fernández-Pérez, L. Fernández-Mérida, J. Santana, R. Souto, Imaging local surface reactivity on stainless steels 304 and 316 in acid chloride solution using Scanning electrochemical microscopy and the scanning vibrating electrode technique, *Electrochim. Acta* 134 (2014) 167–175.
- [8] J. Izquierdo, L. Martín-Ruiz, B. Fernández-Pérez, R. Rodríguez-Raposo, J. Santana, R. Souto, Scanning microelectrochemical characterization of the effect of polarization on the localized corrosion of 304 stainless steel in chloride solution, *J. Electroanal. Chem.* 728 (2014) 148–157.
- [9] N. Aouina, F. Balbaud-Célérier, F. Huet, S. Joiret, H. Perrot, F. Rouillard, V. Vivier, Single pit initiation on 316L austenitic stainless steel using scanning electrochemical microscopy, *Electrochim. Acta* 56 (24) (2011) 8589–8596.
- [10] K. Eckhard, M. Etienne, A. Schulte, W. Schuhmann, Constant-distance mode AC-SECM for the visualisation of corrosion pits, *Electrochem. Commun.* 9 (7) (2007) 1793–1797.
- [11] Y. Yin, L. Niu, M. Lu, W. Guo, S. Chen, In situ characterization of localized corrosion of stainless steel by scanning electrochemical microscope, *Appl. Surf. Sci.* 255 (22) (2009) 9193–9199.
- [12] A. Bastos, A. Simoes, S. González, Y. González-García, R. Souto, Imaging concentration profiles of redox-active species in open-circuit corrosion processes with the scanning electrochemical microscope, *Electrochem. Commun.* 6 (11) (2004) 1212–1215.
- [13] W. Liu, F. Cao, Y. Xia, L. Chang, J. Zhang, Localized corrosion of magnesium alloys in NaCl solutions explored by scanning electrochemical microscopy in feedback mode, *Electrochim. Acta* 132 (2014) 377–388.
- [14] D. Filotás, B. Fernández-Pérez, J. Izquierdo, L. Nagy, G. Nagy, R. Souto, Novel dual microelectrode probe for the simultaneous visualization of local  $\text{Zn}^{2+}$  and pH distributions in galvanic corrosion processes, *Corros. Sci.* 114 (2017) 37–44.
- [15] D. Filotás, B. Fernández-Pérez, J. Izquierdo, A. Kiss, L. Nagy, G. Nagy, R. Souto, Improved potentiometric SECM imaging of galvanic corrosion reactions, *Corros. Sci.* 129 (2017) 136–145.
- [16] A. Kiss, D. Filotás, R. Souto, G. Nagy, The effect of electric field on potentiometric scanning electrochemical microscopic imaging, *Electrochem. Commun.* 77 (2017) 138–141.
- [17] N.D. Budiansky, F. Bocher, H. Cong, M. Hurley, J.R. Scully, Use of coupled multi-electrode arrays to advance the understanding of selected corrosion phenomena, *Corrosion* 63 (6) (2007) 537–554.
- [18] L. Yang, N. Sridhar, C.S. Brossia, D.S. Dunn, Evaluation of the coupled multi-electrode array sensor as a real-time corrosion monitor, *Corros. Sci.* 47 (7) (2005) 1794–1809.
- [19] L. Yang, N. Sridhar, O. Pensado, D. Dunn, An in-situ galvanically coupled multi-electrode array sensor for localized corrosion, *Corrosion* 58 (12) (2002) 1004–1014.
- [20] D. Filotás, B. Fernández-Pérez, A. Kiss, L. Nagy, G. Nagy, R. Souto, Double barrel microelectrode assembly to prevent electrical field effects in potentiometric SECM imaging of galvanic corrosion processes, *J. Electrochem. Soc.* 165 (5) (2018) C270–C277.